Fluorescent Oligonucleotides and Deoxynucleotide Triphosphates: Preparation and Their Interaction with the Large (Klenow) Fragment of *Escherichia coli* DNA Polymerase I

Dwayne J. Allen, Paul L. Darke, and Stephen J. Benkovic*

Department of Chemistry, 152 Davey Laboratory, The Pennsylvania State University, University Park, Pennsylvania 16802

Received December 9, 1988; Revised Manuscript Received February 21, 1989

ABSTRACT: Fluorescent derivatives of short oligonucleotides of defined sequence were prepared by the incorporation of 5-(propylamino)uridine via current phosphoramidite chemistry, followed by derivatization of the propylamine function with mansyl chloride. These oligomers, annealed to complementary oligomers, yielded short duplex DNA fluorescently labeled at a specific base. The fluorescence emission from this labeled duplex increases upon binding to the Klenow fragment of DNA polymerase I (KF) at specific positions within the duplex DNA. By varying the position of the label within the duplex DNA and observing the emission, points of strong enzyme–DNA interactions were elucidated. A similar fluorescent derivative of a deoxynucleoside triphosphate (dNTP), 5-[[[[[[(5-sulfonaphthalenyl)amino]ethyl]amino]carbonyl]-methyl]thio]-2′-deoxyuridine 5′-triphosphate (AEDANS-S-dUTP), was synthesized, whose emission also was increased upon binding to KF. The change in emission intensities between unbound and bound substrates enabled the measurements of K_Ds for the DNA and dNTP derivative, which were found to be 0.15 nM and 2.9 μM, respectively. Stopped-flow measurements on these species yielded association and dissociation rates for each. Anisotropy measurements of the labeled base at various positions in the duplex yielded values that support the measurements made by observing the emission intensities.

Escherichia coli DNA polymerase I (pol I) is a multifunctional enzyme responsible for DNA repair and replication in vivo (Kornberg, 1980). The enzyme's polymerase activity, which catalyzes the template-directed extension of a primer DNA strand, and the separate 3′→5′ and 5′→3′ exonuclease activities are all found on a single 103-kDa polypeptide chain (Jovin et al., 1969). Treatment of pol I by subtilisin produces two peptides; the larger is termed the Klenow fragment and contains the polymerase and 3′→5′ exonuclease activities (Klenow et al., 1970; Brutlag et al., 1969). The use of the Klenow fragment avoids any complications arising due to the 5′→3′ exonuclease activity in studies of the accurate replication of synthetic DNA templates (Kuchta et al., 1987). Presently, were are attempting to relate this functional description of Klenow fragment to the detailed crystal structure of the enzyme (Ollis et al., 1985).

The crystal structure, determined in the absence of duplex DNA, shows that the protein consists of two distinct domains. The larger domain contains a deep cleft, into which duplex DNA can be fit through model building. The polymerase activity is believed to reside at one end of the cleft, near the interdomain linkage, while the 3′→5′ exonuclease site is found on the smaller domain. Co-crystals of DNA–KF have been difficult to obtain (Joyce & Steitz, 1987), and in an attempt to aid in the structural understanding of this enzyme, fluorescent analogues of duplex DNA and deoxynucleoside triphosphates were synthesized. The fluorophores, aminonaphthalenesulfonate derivatives, are quite environmentally sensitive and have been useful in determining protein contacts (Onodera et al., 1976). In the present studies, DNA duplexes of defined sequence that contain a fluorescently modified 5-(propylamino)uridine in a known position were used to determine which points on the duplex were in close contact with the enzyme. The fluorescence emission increase of the fluorophore upon close contact with the enzyme enabled the determination of association and dissociation rates of duplex DNA and deoxynucleotide triphosphates to KF.

Experimental Procedures

Materials. Klenow fragment was purified from *E. coli* CJ333 according to the method of Joyce and Grindley (1983). The *E. coli* strain was kindly provided by Professor C. Joyce. Polyacrylamide gel electrophoresis of the purified enzyme indicated at least 99% homogeneity. Protein concentrations were determined spectrophotometrically with $\epsilon_{278} = 6.22 \times 10^7$ M^{-1} cm^{-1} (Setlow et al., 1972). Polymerase activity was measured with the DE-81 filter paper assay (Bryant et al., 1983). Mansyl[1] chloride and dansyl chloride were from Molecular Probes. 5′-(Dimethoxytrityl)-3′-methylphosphoramidites were from American Bionetics. Nucleotide triphosphates were from Sigma. [γ-^{32}P]ATP (>3000 Ci/mmol) was from New England Nuclear. Acetonitrile and triethylamine were from Aldrich. All other reagents were of the highest quality commercially available.

Synthesis of AEDANS-S-dUTP. The method of Ho et al. (1978) was used to synthesize bis[5-(2′-deoxyuridine 5′-phosphate)] disulfide (bis-5dUMP), which was obtained in 79% yield after purification on DEAE-Sephadex A-25. The oxidized bismonophosphate eluted at 0.18 M TEAB from a

* Author to whom correspondence should be addressed.

[1] Abbreviations: AEDANS-S-dUTP, 5-[[[[[[(5-sulfonaphthalenyl)-amino]ethyl]amino]carbonyl]methyl]thio]-2′-deoxyuridine 5′-triphosphate; dansyl, 5-(dimethylamino)naphthalene-1-sulfonate; dNTP, deoxynucleotide triphosphate; IAEDANS, *N*-[[(iodoacetyl)amino]-ethyl]-5-naphthylamine-1-sulfonic acid; HPLC, high-pressure liquid chromatography; HOAc, acetic acid; mansyl, 6-(*N*-methylanilino)-naphthalene-2-sulfonate; TEAA, triethylammonium acetate; TEAB, triethylammonium bicarbonate; Tris, tris(hydroxymethyl)aminomethane.

0006-2960/89/0428-4601$01.50/0

0.56 × 22 cm column washed with a 5–300 mM TEAB linear gradient. The UV spectrum has an absorption maximum at 272 nm (pH 8.0), which upon the addition of dithiothreitol changes to 333 nm.

Pyrophosphorylation of the monophosphate (297 μmol) was achieved by the morpholidate method (Moffatt, 1964). The triphosphate was purified on DEAE-cellulose (2.4 × 33 cm) with a 200–500 mM TEAB gradient (1.8 per side) and eluted as the oxidized disulfide at 0.36 M TEAB. The yield was 64 μmol (21%). The bistriphosphate compound was not completely resolved from the monophosphate–triphosphate mixed disulfide after purification, as judged by ^{31}P NMR performed with and without added dithiothreitol. Subsequent sulfhydryl modifications after reduction of the disulfide, followed by purification, yielded the separate mono- and triphosphates.

The triphosphate disulfide (15 μmol) was dried from ethanol solution as the triethylammonium salt under a stream of argon and then taken into 750 μL of degassed 50 mM potassium phosphate (pH 7.5). Dithiothreitol (15 μmol) in 15 μL was added and the solution kept under argon. After 20 min at room temperature, 94 μL of IAEDANS in the same buffer (18.7 μmol) was added. After 2 h, the solution was diluted to 100 mL and applied to a 1.4 × 20 cm DEAE-cellulose column. After washing with 50 mL of 50 mM TEAB, a gradient of 50–500 mM TEAB eluted the triphosphate adduct, AEDANS-S-dUTP, at 200 mM TEAB. Yield was 9 μmol (60%). Phosphorus assay (Eaton et al., 1976) gave 3.0 phosphates per chromophore at 337 nm (ϵ = 5900 M^{-1} cm^{-1}). The ^{31}P NMR spectrum showed a characteristic nucleoside triphosphate pattern (D_2O, pH 9.3 relative to 1 M H_3PO_4); 5.61 (d, γ-P), 10.86 (d, 1 H splitting apparent, α-P), 21.51 (t, β-P). ^1H spectrum (D_2O, relative to DSS): δ 8.12 (d, 1 H), 8.00 (s, 1 H, 6-H of uracil), 7.98 (d, 1 H), 7.93 (d, 1 H), 7.53 (m, 2 H), 6.81 (d, 1 H), 5.40 (dd, 1 H, 1′-H), 4.44 (m, 1 H, 3′-H), 4.21 (m, 2 H), 4.04 (m, 1 H, 4′-H), 3.72 (m, 2 H), 3.61 (t, 2 H), 3.41 (t, 2 H), 2.46 (m, 2 H, 2′-H).

Synthesis of Oligonucleotides. Template 20-mer, primer 9-mer, and primer 20-mer (Figure 1) were synthesized on an Applied Biosystems DNA synthesizer Model 380A. Methylphosphoramidite chemistry was used. The 5′-OH tritylated oligomer was purified on a reverse-phase C-18 HPLC column (Altex). A gradient was run from 10% acetonitrile/90% 100 mM TEAA, pH 7.0 (solvent A), to 100% acetonitrile (solvent B) at 1% solvent B/min following a 4-min isocratic step of solvent A. The collected oligomer was lyophilized and dissolved in 6% HOAc and kept at room temperature for 30 min to remove the dimethoxytrityl group. The deblocked oligomer was repurified by HPLC using the same conditions used for the tritylated oligomer.

Primer 11-mer (Figure 1) and template 30-mer were also synthesized on an Applied Biosystems DNA synthesizer Model 380A using methyl phosphoramidite chemistry. At specified positions in the oligomers, a derivatizable phthalimide-protected 5-(aminopropyl)-2′-deoxyuridine 3′-(methyl diisopropylphosphoramidite) (Gibson, et al., 1987) was used in place of the normal methyl phosphoramidites. These oligomers were derivatized before purification.

Derivatization of Oligonucleotides. To 40 nmol of either 11-mer or 30-mer (assumed ϵ = 10 000 M^{-1} cm^{-1} per base) in 200 mM TEAB, pH 10 (400 μL), was added 1 μmol of mansyl or dansyl chloride in acetone in 18 μL. The reaction was performed at room temperature in the dark. After 6 h, another 18 μL of the above acid chloride solution was added and the reaction allowed to proceed for another 12 h. A precipitate formed, which was removed by centrifugation, and the resulting supernatant was purified by reverse-phase C-18 HPLC as described above. The labeled oligomers were identified by the association of a UV absorbance at 340 nm (mansyl or dansyl group) with the 260-nm absorbance of the oligonucleotide. Purified labeled tritylated oligomers were deblocked at the 5′-OH with 6% HOAc as above and repurified.

Formation of Fluorescent Duplexes. Fluorescent duplexes were prepared by the addition of equimolar amounts of either labeled primer or template with their unlabeled complementary strand in a buffer of 50 mM Tris-HCl, pH 7.4.

Titration of Labeled 11/20-mer with Klenow Fragment.* To a 1.0-mL solution containing 317 pmol of 11*/20-mer (dansyl labeled), 50 mM Tris-HCl, pH 7.4, and 3 mM $MgCl_2$ were added aliquots (2 μL of 32 μM) of Klenow fragment. The solution's fluorescence emission, measured on an SLM 8000C spectrofluorometer, was measured by using an excitation of 340 nm. Aliquots were added until no further emission intensity change was observed. The concentration of the dansyl-labeled 11-mer was determined by 5′-OH labeling with ^{32}P and DE-81 filter binding assay.

Incorporation of AEDANS-S-dUTP into Oligonucleotide Duplex. Primer 9-mer and template 20-mer were 5′-OH labeled by using [γ-^{32}P]ATP and T4 polynucleotide kinase (Mizrahi et al., 1986). Reactions were performed by the combination of 2 μL each of the primer and template labeling reactions followed by the addition of 2 μL of a Klenow fragment/AEDANS-S-dUTP solution. Final concentrations used were 300 nM oligonucleotide, 500 μM Klenow fragment, and 50 μM AEDANS-S-dUTP. Following a 15-min reaction time, solutions of dNTP were added. Reactions were quenched into sequence loading buffer 10 min after additions of the dNTP solutions. Oligonucleotide products were visualized by autoradiography after gel electrophoresis on a 15% denaturing polyacrylamide sequencing gel.

Stepwise Elongation of 11/20-mer.* To a 1.0-mL solution containing 317 pmol of 11*/20-mer 50 mM Tris-HCl, pH 7.4, 3 mM $MgCl_2$, and 350 pmol of Klenow fragment was added stepwise 3.3 μL (10 mM) of dCTP, dATP, dGTP, and dTTP. The solution's fluorescence emission, excited at 340 nm, was measured following each addition of dNTP.

Anisotropy Measurements of Labeled Oligonucleotides. Anisotropy measurements of labeled oligomers were made on an SLM 8000C spectrofluorometer using the T-format method. Filters used were 408-nm cutoff and were purchased from SLM. Measurements were taken on a 1.0-mL solution containing 110 pmol of labeled oligonucleotide duplex. Klenow fragment was added as well as the appropriate dNTPs so that differing primer lengths could be observed.

Titration of AEDANS-S-dUTP with Klenow Fragment. To a 1.0-mL solution containing 500 pmol of AEDANS-SdUTP, 50 mM Tris-HCl, pH 7.4, and 3 mM $MgCl_2$ were added aliquots of Klenow fragment. The solution's fluorescence emission was measured by using an excitation wavelength of 340 nm.

Transient Kinetics. Pre-steady-state kinetics data were obtained by using a stopped-flow apparatus operating in the fluorescence mode, which was built by Professor K. A. Johnson (Johnson, 1986) and possesses a 1.6-ms dead time, a 2-mm path length, and a thermostated sample cell. Interference filters (Ditric Optics) were used on both the light input (excitation) and output (emission). The formation or dissociation of the enzyme complexes was followed by using a 340-nm interference filter on the excitation input and then monitoring the increase or decrease in fluorescence with an output filter

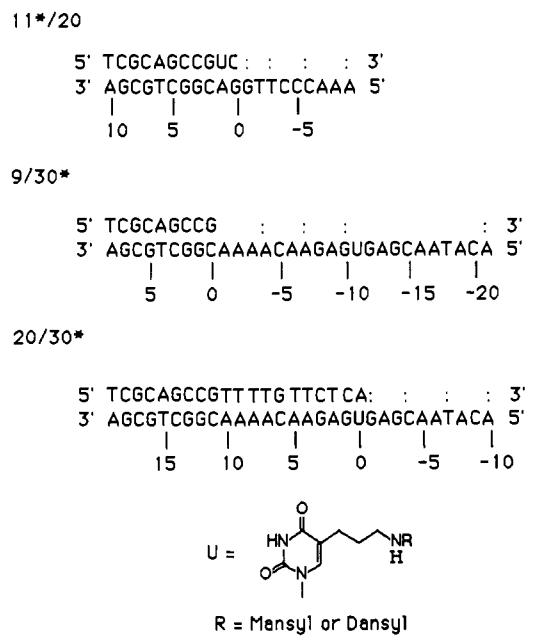

FIGURE 1: Fluorescent duplex systems. U denotes a derivatizable base, modified with amino selective fluorophores as described under Experimental Procedures. The primers in the duplex systems can be sequentially elongated with Klenow fragment and appropriate dNTPs. The colon denotes the length of the elongated primer in the absence of the next required dNTP.

at the emission wavelength of 450 nm, for mansyl-labeled oligonucleotide duplex, or 530 nm for AEDANS-S-dUTP.

Data were collected by a computer over a given time interval following a trigger impulse, until a few milliseconds before stop, and stored on a floppy disk. The data were then graphically displayed and analyzed by using a single-exponential model

$$F(t) = \text{AMP} \exp(-k_{obs}t) + \text{base line}$$

where $F(t)$ is the observed fluorescence at time t, AMP is the fluorescence amplitude for the fluorescence change, and k_{obs} is the observed rate constant.

For the association reaction of Klenow fragment to the mansyl-labeled oligonucleotide duplex (11*/20), the final concentration of duplex was 25 nM and the concentration of Klenow fragment was varied from 250 nM to 1.0 μM. In the association reaction of Klenow fragment to AEDANS-S-dUTP, the final concentration of AEDANS-S-dUTP was 300 nM and the final concentration of Klenow fragment was varied from 1.0 to 4 μM. In both association reactions, the increase in fluorescence signal was monitored.

For the dissociation of the Klenow-fragment-labeled duplex complex, final concentrations of 150 nM Klenow fragment and 100 nM mansyl-labeled duplex were used. The dissociated labeled duplex was diluted into salmon sperm DNA, whose final base concentration was varied between 1.0 and 2.0 mM (assuming average ϵ = 10 000 M^{-1} cm^{-1} for each base). For the dissociation of the Klenow fragment–AEDANS-S-dUTP complex, final concentrations of 2 μM Klenow fragment and 10 μM AEDANS-S-dUTP were used. The dissociated AEDANS-S-dUTP was diluted into dNTPs at a final concentration of 2 mM. In both dissociation reactions, the decrease in fluorescence signal was monitored.

The fluorescence signal decrease upon elongation of 11*/20-mer to 12*/20-mer (incorporation of dCTP) was used to monitor the rate of this elongation. The final concentration of Klenow fragment was 150 nM, and the final concentration of 11*/20 was 100 nM. The final concentration of dCTP was varied between 10 and 60 μM.

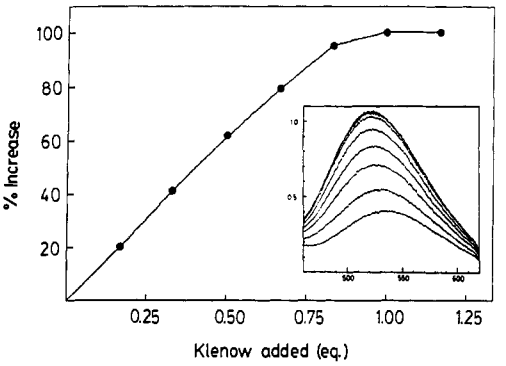

FIGURE 2: Titration of dansyl-labeled 11*/20-mer with Klenow fragment. Aliquots of Klenow fragment were added to a 319 μM solution of labeled 11*/20-mer, and the fluorescence emission increase from the dansyl fluorophore was followed by using an excitation of 340 nm.

Table I: Fluorescence Parameters as a Function of the Fluorophore Position in the 11*/20-mer KF Complex (Dansyl Labeled)

dNTP added	fluorescence intensity	peak max (nm)	probe position	anisotropy
–	2.6	524	+1	0.2199
C	1.7	530	+2	0.1980
CA	1.7	533	+4	0.1995
CAG	1.0	539	+7	0.1659
CAGT	1.0	539	+10	0.1623
duplex	1.0	538	+1	0.0776

RESULTS

Duplex Contacts. The addition of Klenow fragment to dansyl-labeled 11*/20-mer (Figure 1) caused the fluorescence emission from the labeled duplex to increase 2.6-fold (Figure 2). The peak maximum in the presence of Klenow fragment is blue-shifted 14 nm, from 538 to 524 nm, indicating that the fluorophore's environment is more hydrophobic relative to the aqueous solvent. The increase in the emission of the labeled duplex is complete when 1.0 equiv of enzyme has been added, indicating that the enzyme binds only 1 equiv of duplex. Identical results were obtained with mansyl-labeled 11*/20-mer (data not shown). The fluorescence increase with the mansyl-labeled 11*/20-mer is 6.8-fold, and the peak maximum blue shift is 14 nm, from 461 to 447 nm. The increased sensitivity of the mansyl group emission intensity, relative to that of the dansyl group, upon binding to Klenow fragment made the mansyl group more attractive for observing these interactions. For this reason, further experiments were performed on mansyl-labeled systems.

The template in the 11*/20 system is designed so that the addition of appropriate dNTPs will elongate the 11*-mer in discrete steps, placing the fluorophore a known number of base pairs away from the DNA primer-terminus. The design of the template enables the fluorophore to be located at positions +1, +2, +4, +7, and +10. The numbering system used defines the primer-terminus as 0. Other positions are assigned a numerical value equivalent to their distance, in bases, from the primer-terminus, with positions in the duplex region assigned a positive value and those in the single-stranded region a negative value. As the primer 11*-mer is lengthened, there is a decrease in the fluorescence emission intensity as well as an associated red shift of the peak maxium, indicating that the fluorophore is moving into a more hydrophilic environment (Table I). When the fluorophore is at position +2 or +4, the fluorescence emission intensity of the duplex is 1.7 times greater than that of the duplex with no added Klenow frag-

Table II: Fluorescence Parameters as a Function of the Fluorophore Position in the 9/30*-mer KF Complex (Mansyl Labeled)

dNTP added	fluorescence intensity	peak max (nm)	probe position	anisotropy
-	6.3	439	-11	0.2699
T	3.4	447	-7	0.2511
TG	5.3	444	-4	0.2678
TGC	4.8	445	0	0.2694
TGCA	3.0	445	+10	0.2442
duplex	1.0	466	-11	0.1745

Table III: 20/30*-mer Data (Mansyl Labeled)

dNTP added	fluorescence intensity	peak max (nm)	probe position	anisotropy
-	6.3	444	0	0.2933
C	4.6	447	+1	0.2869
CT	3.7	443	+3	0.2786
CTG	2.9	442	+6	0.2613
CTGA	2.9	459	+10	0.2515
duplex	1.0	459	0	0.1990

ment. At position +7 or +10, the fluorophore's emission intensity is equal to that of the duplex with no added Klenow fragment. Also, at these positions the wavelength of the peak maximum is equal to that of the labeled duplex alone.

The data suggest that there are strong protein–DNA interactions near the primer-terminus (+1) that are still significant several bases away in the duplex region (positions +2 and +4). These contacts are not detected further into the duplex region (positions +7 and +10). We conclude that the enzyme binds between 5 and 8 base pairs of the duplex region.

The anisotropy of the fluorophore, indicative of the freedom of rotation, also was measured with the 11*/20-mer as a function of the probe's position in the duplex. As was observed with fluorescence emission, the anisotropy of the duplex changes greatly when bound to Klenow fragment. As the primer is elongated and the probe is moved deeper into the duplex region, the anisotropy decreases as the probe becomes more motile (Table I). The values support the pattern seen for the emission, although the values at positions +7 and +10 are greater than that value for the duplex in the absence of enzyme. It is possible that the higher anisotropy values at these positions are due to the fact that the fluorophore is flanked by several base pairs on either side, constraining its freedom to rotate relative to being located near the 3'-OH end. The placement of the probe in the interior regions of a 30-mer (Figure 1, 9/30*, 20/30*), without added Klenow fragment, produced anisotropy values similar to those observed at positions +7 and +10 for the 11*/20-mer bound to the enzyme (Tables II and III, duplex alone).

Single-Strand Contacts. To observe protein–DNA interactions in the single-strand region of a primer-template system, the mansyl-derivatized uridine was placed 11 bases upstream from the primer-terminus. Using the probe in this position and the 9-mer (Figure 1) as a primer, the increase in the fluorophore's emission intensity in the template was followed as the probe approached the primer-terminus when bound to the polymerase. Again, the template was designed so that the primer could be elongated stepwise by the addition of appropriate dNTPs. Using the 9-mer as a primer, the positions occupied by the fluorophore relative to primer-terminus would be -11, -7, -4, -1, and +10. Upon addition of Klenow fragment to the mansyl-labeled 9/30* system, the fluorescence emission intensity increased 6.3-fold, accompanied by a blue shift in the peak maximum from 466 to 439 nm. The emission intensities for all positions are given in Table II. The use of a different primer (20-mer, Figure 1), enabled the observation of emission intensities as the fluorophore attached to the template strand moved through the duplex region upon the addition of the appropriate dNTPs. The positions occupied by the fluorophore relative to the primer would be 0, +1, +3, +6, and +10. The fluorescent parameters obtained are shown in Table III.

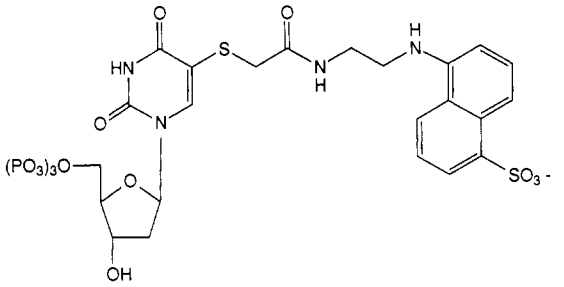

AEDANS-S-dUTP

FIGURE 3: Structure of AEDANS-S-dUTP.

By use of the mansyl-labeled 9/30* and 20/30* systems, the anisotropy of the fluorophore in the single strand was observed at the same positions used to observe the fluorescence emission. The results shown in Tables II and III closely resemble the results obtained by monitoring the emission. The strongest interactions with the enzyme are at position -11 and at the primer-terminus. In both the emission and anisotropy experiments, there is still substantial interaction with the enzyme at position +10 when the fluorophore is located in the template strand. This was not observed in the 9*/20 system, when the fluorophore is located on the opposite strand.

Measurements of Association/Dissociation Rates for Fluorophores. Upon binding to Klenow fragment, the emission intensity of AEDANS-S-dUTP (Figure 3) increases 3.7-fold and the peak maximum shifts 13 nm, from 494 to 481 nm. A nonlinear fit of the titration curve produced a K_D of 2.2 μM. The fluorescence emission increase observed upon AEDANS-S-dUTP binding to Klenow fragment can be decreased upon addition of a large excess of dNTPs, indicating that the AEDANS-S-dUTP is binding in the triphosphate site of the enzyme. In the presence of 9/20-mer this probe can be incorporated into the duplex (Figure 4).

Since there are large changes in the fluorescence emission of both mansyl-labeled 11*/20-mer and AEDANS-S-dUTP upon binding to Klenow fragment, these changes were used to observe the rate of binding by measuring the increase in substrate fluorescence as a function of time after mixing of the enzyme with a ligand in a stopped-flow apparatus. In the formation of binary complexes with either mansyl-labeled 11*/20-mer or AEDANS-S-dUTP, single-exponential increases in the fluorescence signal were observed. This observation is simply explained as the association of the ligand with the enzyme to form the binary complex.

$$E + L \rightleftharpoons EL$$

The observed first-order rate constants for the association rates of both 11*/20-mer and AEDANS-S-dUTP increase linearly with enzyme concentration, showing no signs of saturation. For a simple association reaction, the observed rate constant under pseudo-first-order conditions may equal

$$k_{obs} = k_{on}[E] + k_{off}$$

where k_{on} and k_{off} are the association and dissociation rate constants, respectively. Linear plots of k_{obs} vs varying con-

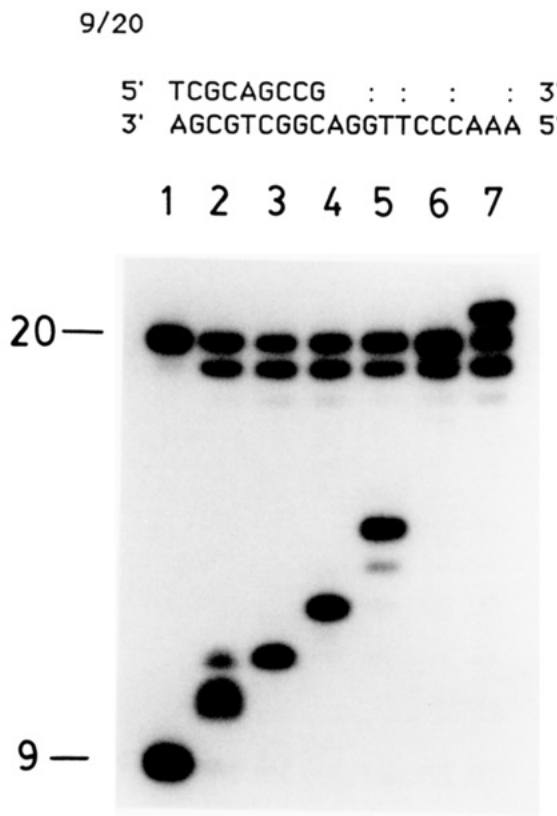

FIGURE 4: AEDANS-S-dUTP incorporation into a 9/20 oligonucleotide duplex system. Both the 9-mer and 20-mer were 5'-OH-labeled with ^{32}P. (Lane 1) 9-mer and 20-mer. (Lane 2) 9/20 duplex elongated with dTTP. (Lanes 3–8) 9/20 duplex elongated with AEDANS-S-dUTP followed by the addition of dNTPs: (lane 4) dC; (lane 5) dC, dA; (lane 6) dC, dA, dG; (lane 7) dC, dA, dG, dT.

Scheme I

$$E^*L1 \underset{k_{fwd}}{\overset{k_{rev}}{\rightleftharpoons}} E + L1$$

$$E + L2 \underset{k_{diss}}{\overset{k_{trap}}{\rightleftharpoons}} E^*L2$$

centrations of Klenow fragment yielded rate constants for the binding of 11*/20-mer (5.5×10^8 M^{-1} s^{-1}) and AEDANS-S-dUTP (7.6×10^7 M^{-1} s^{-1}).

The dissociation rate constant of a ligand from an enzyme–ligand complex (EL1) can be measured through trapping by a second ligand (L2), which competes for the same binding site (Scheme I). In this technique, the first enzyme–ligand complex (EL1), with an increased fluorescence emission, is mixed with a large excess of a second ligand (L2), which is nonfluorescent and competes for the same binding site. The formation of the new complex, EL2, is monitored by the decrease in the fluorescence emission intensity as bound ligand (EL1) dissociates to free ligand (L1). When $k_{rev} \ll k_{trap}[L2] \gg k_{fwd}[L1]$, the fluorescence change is attributable to the conversion of EL1 to EL2 characterized by a single exponential with the dissociation rate constant (k_{rev}) for L1. The validity of these conditions is checked by showing that k_{obs} for this reaction is independent of the concentration of the trapping ligand, L2.

As shown in Figure 5, for the measurement of the dissociation of AEDANS-S-dUTP from Klenow fragment by trapping with dNTP, the observed decrease in the fluorescence

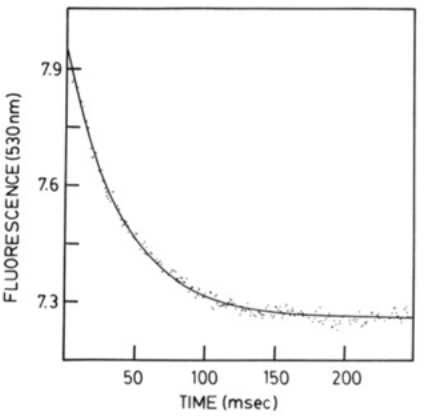

FIGURE 5: Time course of enzyme-bound AEDANS-S-dUTP fluorescence decay upon mixing of Klenow fragment/AEDANS-S-dUTP into a pool of competing dNTP. All four dNTPs were used with no significant change observed in the dissociation rate of AEDANS-S-dUTP from Klenow fragment. Data were collected into 250 memory points and were fit to a single-exponential model.

signal is well described by fitting to a single-exponential decay. Competition by the four triphosphates dATP, dGTP, dCTP, and dTTP showed no significant difference between the observed rates (230 ± 10 s^{-1}).

The measurement of the dissociation of mansyl-labeled 11*/20-mer from Klenow fragment was observed by trapping with an excess of salmon sperm DNA. The observed decrease in fluorescence signal upon dissociation likewise was described by a single exponential. Increasing the concentration of the trap DNA had no effect on the observed rate constant of 0.85 s^{-1} for dissociation of the 11*/20-mer from KF.

As noted in the 11*/20-mer elongation experiments, there is a significant decrease in the fluorescence signal when the primer 11-mer is elongated to a 12-mer by the incorporation of dCTP. This fluorescence decrease is well described by a single exponential with a rate constant of 1.5 s^{-1}. The observed rate of incorporation of dNTP into unmodified oligonucleotide duplexes has been shown to be 50 s^{-1} (Kuchta et al., 1987), significantly more rapid than the rate observed upon dCTP incorporation in the 11*/20 system described here.

Discussion

E. coli DNA polymerase I (pol I) and calf thymus terminal deoxynucleotidyl transferase (TdT) have been shown to utilize uridine nucleotides substituted at the 5-position as substrates (Dale et al., 1973). The structure of B-DNA is such that a linking arm from the 5-position of a base-paired uracil to a fluorophore should extend into the major groove with minimal distortion of the helix. A fluorescent DNA duplex was synthesized by the incorporation of a derivatizable uridine analogue, modified at the 5-position, into a primer oligonucleotide. Following modification with an amine selective fluorophore, the modified primer was annealed to a corresponding template strand to give fluorescent duplex DNA. Due to the nature of the phosphoramidite chemistry used, the derivatizable base was placed 1 base away from the primer-terminus in the duplex region. The fluorophore of choice for labeling the DNA was mansyl chloride since the resulting sulfonamide is very environmentally sensitive. The sulfonamide derived from dansyl chloride, although a smaller fluorophore, was not as sensitive.

The binding of fluorescently labeled duplex DNA to Klenow fragment produced an increase in the emission of the fluorophore. For the dansyl-labeled DNA, this increase was 2.6-fold, whereas that of the mansyl-labeled DNA was 6.8-fold. In both cases, the observed blue shift observed of the peak maximum

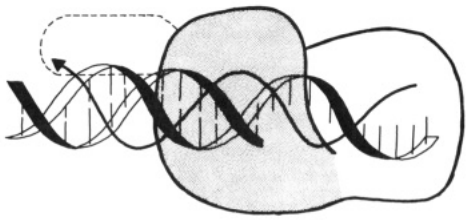

FIGURE 6: Model of Klenow fragment with bound oligonucleotide duplex. Arrow traces the DNA major groove through the duplex. Dashed area indicates a region where 50 disordered amino acids are thought to reside.

was 14 nm, and the emission increase was complete when 1 equiv of enzyme had been added, indicating that the enzyme binds one molecule of duplex DNA per molecule of enzyme. The template is so designed that the addition of appropriate dNTPs will move the fluorescently labeled base into the duplex region in discrete steps. As the fluorophore is moved into the duplex region of DNA, the increase in the emission or change in anisotropy observed upon polymerase binding is reduced and completely lost when the fluorophore is between 5 and 8 bases within the duplex region. The extent of duplex interaction with the enzyme from these experiments is in agreement with previous footprinting experiments with Klenow fragment (C. Joyce, personal communication).

Single-stranded contact points in the single-stranded template region were investigated by the placement of the mansyl-labeled uridine 11 bases upstream from the primer-terminus. Interaction leads to two maxima in the fluorescent emission spectra, one at position −11, and a second at position −4. At the primer-terminus, as would be expected, the interaction with the enzyme was very strong but again decreased as the fluorophore was moved into the duplex region. The emission minimum that occurs at position −7 (Table II) may suggest a helical property of the single-stranded template bound to the enzyme (Figure 6). The template, bound in a helical form, would have a strong protein–DNA interaction at position −11, which would be diminished at position −7 as the template curled away from the enzyme. At position −4, the template would be interacting with the DNA binding cleft, giving rise to an increased interaction. In contrast to when the fluorophore was located in the primer strand, the emission of the probe on the template was still increased 3-fold relative to labeled duplex DNA in the absence of enzyme when the fluorophore was located 10 bases within the duplex region. This difference may be attributed to an interaction with the 50 amino acids that extend from the top of the DNA binding cleft but do not appear in the crystal structure owing to their disorder (Ollis et al., 1985). In this model, as the DNA duplex exits the DNA binding cleft, the primer strand extends away and does not contact the disordered amino acid region. Anisotropy measurements, indicating the fluorophore's ability to rotate during the fluorophore's excited-state lifetime, were in close agreement with the results obtained by observing the emission intensities of the fluorophore. When bound to the enzyme, the fluorophore's rational mobility is hindered, resulting in a higher anisotropy value. These increased values corresponded to those positions in the DNA at which the emission intensities were increased, supporting the proposed model for the complex.

A fluorescent nucleotide analogue substituted at the 5-position, AEDANS-S-dUTP, proved useful in studying the binding of a deoxynucleoside triphosphate to the enzyme. The dansyl fluorophore for the triphosphate analogue was chosen because of the environmental sensitivity of its emission and its relatively small size as compared to other commercially available fluorophores. AEDANS-S-dUTP was shown to be a substrate for the Klenow fragment and was incorporated into the 9/20 duplex system and served as an effective primer-terminus as judged by the further incorporation of dNTPs. Upon binding to the Klenow fragment, AEDANS-S-dUTP exhibited a large increase in its emission intensity with a concurrent blue shift in its peak maximum, indicative of the fluorophore moving into a more hydrophobic environment. The addition of the aminonaphthalenesulfonate moiety to the deoxyuridine triphosphate resulted in enhancement of binding (K_D = 2.9 μM) over unlabeled triphosphates, which have dissociation constants ranging from 33 to 147 μM (Englund et al., 1969), while not introducing significant non-site-specific binding.

The large fluorescence changes observed in the binding and dissociation of both the labeled triphosphate and DNA enabled the measurement of the association and dissociation rates for these ligands. The association rates for the labeled triphosphate and DNA were both probably diffusion limited with k_{on} values of 7.6×10^7 and 5.5×10^8 M^{-1} s^{-1}, respectively. The dissociation constant for AEDANS-S-dUTP from KF was measured by a competition method with $k_{off} = 230 \pm 10$ s^{-1}. The measured association and dissociation constants enable the calculation of a K_D = 2.9 μM for AEDANS-S-dUTP bound to Klenow fragment, in good agreement with a measured value of K_D = 2.2 μM, suggesting a single binding step for the nucleotide. Furthermore, this value is similar to those for dNTP binding to binary KF·DNA complexes (Kuchta et al., 1987).

In contrast, the dissociation constant for labeled DNA (mansyl-labeled 11*/20-mer) of 0.085 s^{-1} yields a K_D for the labeled DNA of 0.15 nM. This measured K_D is substantially lower than the 5 nM measured on a unlabeled system (Kuchta et al., 1987) and is probably due to a decreased rate of dissociation owing to the added mansyl fluorophore.

The elongation of the mansyl-labeled 11*/20-mer to a 12*/20 duplex by the incorporation of dCTP produced a decrease in the fluorescence emission of the labeled duplex that was followed by stopped-flow kinetics. The observed rate constant for the emission change of 1.5 s^{-1} is attributed to the movement of the DNA duplex following the chemistry of dCTP incorporation. Since the fluorophore's emission is dependent upon its local environment, this rate might represent translocation to incorporate the next incoming nucleotide, a process that is probably sterically retarded by the presence of the fluorophore as noted above. Thus, these analogues would be most useful for static energy-transfer experiments to measure distances between various substrate sites on Klenow fragment or other polymerases.

References

Brutlag, D., Atkinson, M. R., Setlow, P., & Kornberg, A. (1969) *Biochem. Biophys. Res. Comm. 37*, 982–988.

Bryant, F. R., Johnson, K. A., & Benkovic, S. J. (1983) *Biochemistry 22*, 604–611.

Dale, R. M. K., Livingston, D. C., & Ward, D. C. (1973) *Proc. Natl. Acad. Sci. U.S.A. 70*, 2238–2242.

Eaton, B., & Dennis, E. A. (1976) *Arch. Bioch. Biophys. 176*, 604–609.

Englund, P. T., Huberman, J. A., Jovin, T. M., & Kornberg, A. (1969) *J. Biol. Chem. 244*, 3038–3044.

Gibson, K. J., & Benkovic, S. J. (1987) *Nucleic Acids Res. 15*, 6455–6467.

Ho, Y. K., Novak, L., & Bardos, T. J. (1978) in *Nucleic Acid Chemistry*, pp 813–816, Wiley, New York.

Johnson, K. A. (1986) *Methods Enzymol. 134*, 677–705.

Jovin, T. M., Englund, P. T., & Bertsch, L. L. (1969) *J. Biol. Chem. 24*, 2996–3007.
Joyce, C. M., & Grindley, N. D. F. (1983) *Proc. Natl. Acad. Sci. U.S.A. 80*, 1830–1834.
Joyce, C. M., & Steitz, T. A. (1987) *Trends Biochem. Sci.* 288–292.
Klenow, H., & Henningson, I. (1970) *Proc. Natl. Acad. Sci. U.S.A. 65*, 168–175.
Kornberg, A. (1980) in *DNA Replication*, pp 104–105, Freeman, San Francisco.
Kuchta, R. D., Mizrahi, V., Benkovic, P. A., Johnson, K. A., & Benkovic, S. J. (1987) *Biochemistry 26*, 8410–8417.
Mizrahi, V., Benkovic, P. A., & Benkovic, S. J. (1986) *Proc. Natl. Acad. Sci. U.S.A. 83*, 231–235.
Moffatt, J. G. (1964) *Can. J. Chem. 42*, 599–604.
Ollis, D. L., Brick, P., Hamlin, R., Xuong, N. G., & Steitz, T. A. (1985) *Nature 313*, 762–766.
Onodera, M., Shiokawa, H., & Takagi, T. (1976) *J. Biochem. 79*, 195–201.
Setlow, P., Brutlag, D., & Kornberg, A. (1972) *J. Biol. Chem. 247*, 224–248.

An NMR Study of the Helix V–Loop E Region of the 5S RNA from *Escherichia coli*†

P. Zhang and P. B. Moore*
Department of Chemistry and Department of Molecular Biophysics and Biochemistry, Yale University, New Haven, Connecticut 05611

Received November 21, 1988; Revised Manuscript Received February 13, 1989

ABSTRACT: Experiments are described that complete the assignment of the imino proton NMR spectrum of the fragment 1 domain from the 5S RNA of *Escherichia coli*. Most of the new assignments fall in the helix V–loop E portion of the molecule (bases 70–78 and 98–106), the region most sensitive to the binding of ribosomal protein L25. The spectroscopic data are incompatible with the standard, phylogenetically derived model for 5S RNA, which makes all the base pairs possible in loop E with the sequences aligned in parallel (C70–G106, C71–G105, etc.) [see Delihas et al. (1984) *Prog. Nucleic Acid Res. Mol. Biol. 31*, 161–190]. Furthermore, the alternative loop E model proposed for spinach chloroplast 5S RNA by Romby et al. [(1988) *Biochemistry 27*, 4721–4730] does not apply to the closely homologous 5S RNA from *E. coli*. The 5S RNAs from *E. coli* and spinach chloroplasts do not have the same secondary structures in solution despite their strong sequence homologies, and neither appears to conform to the standard model for 5S RNA in the loop E region.

Figure 1 shows the sequence of the 5S RNA from *Escherichia coli* drawn in the secondary structure derived for it by comparative sequence analysis. Like the larger rRNAs, it is a series of stem–loop structures, and its hydrogen-bonded stems tend to be short and to include non-Watson–Crick base pairs [see Delihas et al. (1984)]. We have been studying this molecule by nuclear magnetic resonance (NMR),[1] concentrating on the portion that resists attack by RNase A, fragment 1 (bases 1–11 and 69–120). Fragment 1 has a three-dimensional structure similar to that of the same sequences in intact 5S RNA, and it binds ribosomal protein L25, the only one of the three 5S binding proteins whose binding site it fully contains (Kime & Moore, 1983a–c).

Fragment 1 includes the helix IV–helix V stem of 5S RNA. Helix IV (bases 79–85 and 91–97) is normal double helix [see Kime and Moore (1983b)], but the secondary structure of the rest of the stem is less obvious. It has two G-C juxtapositions (G106–C70 and G105–C71) at its proximal end, but as one proceeds toward helix IV aligning the strands as shown in Figure 1, only two conventional base pairs can be made. For this reason, there have been differences of opinion about the length of helix V and the size of the unpaired region between helices IV and V (loop E). Nevertheless, helix V and loop E resist enzymatic attack as though they were helical (Kjems et al., 1985), and some archaebacterial 5S RNAs have sequences that permit nearly perfect Watson–Crick pairing in this region (Stahl et al., 1981). Furthermore, the bases of loop E contribute several resonances to the imino proton NMR spectrum of fragment 1, which are particularly conspicuous in complexes of fragment 1 with L25, consistent with the view that loop E is significantly structured (Gewirth et al., 1987). Thus, the helix V–loop E region is shown in Figure 1 heavily hydrogen bonded.

Below we report the results of investigations of ^{15}N-labeled fragment 1 samples in Ca^{2+}-containing buffers at low temperature. Under these conditions, resonances and NOEs can be detected in the free RNA that are not seen in Mg^{2+} at room temperature, the conditions of most of our previous experiments. Most of these "new" resonances represent loop E protons that are also detectable in the spectrum of the fragment 1–L25 complex in Mg^{2+} at room temperature. The new data enable us to complete the assignment of the imino proton spectrum of fragment 1 we began several years ago (Kime & Moore, 1983b). Spectroscopic results on several mutant RNAs

†This work was supported by grants from the National Science Foundation (DMB-860823) and the National Institutes of Health (AI-09167 and GM-22778).

*Address correspondence to this author at the Department of Chemistry, Yale University, 225 Prospect St., New Haven, CT 06511.

[1] Abbreviations: NMR, nuclear magnetic resonance; NOE, nuclear Overhauser effect; poly(U), poly(uridylic acid).

0006-2960/89/0428-4607$01.50/0